

Lawrence Berkeley National Laboratory

Recent Work

Title

Synthesis, Structure, and Selective Gas Adsorption of a Single-Crystalline Zirconium Based Microporous Metal-Organic Framework

Permalink

<https://escholarship.org/uc/item/1w1136pf>

Journal

Crystal Growth and Design, 17(4)

ISSN

1528-7483

Authors

Wang, H
Wang, Q
Teat, SJ
[et al.](#)

Publication Date

2017-04-05

DOI

10.1021/acs.cgd.7b00030

Peer reviewed

Synthesis, Structure, and Selective Gas Adsorption of a Single-Crystalline Zirconium Based Microporous Metal-Organic Framework

*Hao Wang,^a Qining Wang,^a Simon J. Teat,^b David H. Olson^a and Jing Li^{*a}*

^aDepartment of Chemistry and Chemical Biology, Rutgers University, 610 Taylor Road,
Piscataway, New Jersey 08854, United States

^bAdvanced Light Source, Lawrence Berkeley National Laboratory, Berkeley California 94720,
United States.

*Correspondence to: jingli@rutgers.edu

ABSTRACT

Porous metal-organic framework (MOF) materials with high thermal and water stability are desirable for various adsorption based applications. Early transition metal based MOFs such as those built on zirconium metal have been well recognized for their excellent stability toward heat and/or moisture. However, the difficulty of growing large single crystals makes their structural characterizations challenging. Herein we report a porous Zr-MOF, $[\text{Zr}_6\text{O}_4(\text{OH})_4(\text{cca})_6]$ (Zr-cca), which is assembled from zirconium and 4-carboxycinnamic acid (H_2cca) under solvothermal conditions. Single crystal X-ray diffraction analysis reveals the structure of Zr-cca is isoreticular to the prototype zirconium based MOF, UiO-66. Zr-cca shows permanent porosity upon removal of solvent molecules initially residing inside the pores, with a BET surface area of $1178 \text{ m}^2/\text{g}$. As expected, it exhibits good thermal stability (stable up to $400 \text{ }^\circ\text{C}$) and high resistance to acidity over a wide pH range. Evaluation of its gas adsorption performance on various hydrocarbons and fluorocarbons indicates that it preferentially adsorbs C_3 and C_4 hydrocarbons over C_2 analogues. At $30 \text{ }^\circ\text{C}$ Zr-cca takes up more than 50 wt% of perfluorohexane and the adsorption-desorption process is fully recyclable. We have compared this material with UiO-66 and studied the underlying reasons for the difference in their adsorption performance toward perfluorohexane.

INTRODUCTION

Metal-organic frameworks (MOFs) are crystalline materials comprising infinite arrays of nodes (clusters or metal ions) connected by organic ligands.¹ As a new class of multifunctional porous material, MOFs feature high porosity and large degree of tunability. Research on MOFs has focused on their various applications, including gas storage and separation,^{2, 3} catalysis,⁴ sensing,⁵⁻⁷ lighting⁸⁻¹⁰ and so on. While having many advantageous features, a general drawback of MOFs is their relatively poor stability, which cannot be neglected if their use in any of these applications can be realized.^{11, 12} For example, some MOF materials show excellent performance in gas adsorption/separation, surpassing that of traditional porous solid adsorbents, but their poor stability under humid conditions makes it impractical for real applications.¹¹ Over the past few years, tremendous effort has been made to enhance both thermal and water/moisture stability of MOFs which has led to exciting progresses. Incorporation of early transition metals such as zirconium into MOFs has been proven effective in improving their stability.^{13, 14} Compared to widely employed late transition metals such as zinc or copper, zirconium is of higher valence and more oxophilic so that it tends to form stronger Zr-O bonds. Moreover, unlike zinc or copper which commonly exist as mono- or binuclear metal building units in MOFs, zirconium typically formulates into larger secondary building units (SBUs, such as Zr₆ cluster) that generate highly robust MOFs (Zr-MOFs). Since the first group of Zr-MOFs reported in 2008,¹⁴ a large number of new Zr-MOFs have been synthesized and characterized, most of which exhibit excellent thermal/water stability and have been tested for various applications.

The most extensively studied MOF properties and applications are gas adsorption and related gas storage and separation. Continuous progresses have been made in natural gas storage,^{15, 16}

carbon dioxide capture,^{17, 18} hydrocarbons separation,^{2, 19, 20} noble gas purification,²¹⁻²³ to name a few. While early studies focused mostly on hydrogen/methane storage or small gaseous molecule separation, recently there has been an increasing interest in capture and sequestration of harmful volatile organic compounds (VOCs) and fluorocarbons.^{24, 25} Harmful VOCs such as aromatic hydrocarbons are ubiquitous and dangerous to human health and can cause harm to the environment. Even though fluorocarbons exist in low concentrations in the environment, their global warming potentials (GWPs) as greenhouse species are hundreds times higher than that of carbon dioxide.²⁵ MOFs can be promising sorbent materials for the capture of VOCs and fluorocarbons considering their high porosity and tunable functionality. A previous research has shown that a MOF material comprising highly fluorinated organic ligands is capable of adsorbing a large amount of fluorocarbons within a short amount of time due to the specific interaction between fluorinated ligands and fluorocarbons.²⁴

Different from previous studies on fluorocarbon adsorption employing MOFs built of delicate, highly fluorinated ligands or open metal sites,^{24, 26} in this work we design and synthesize an easily-made and highly stable MOF with saturated metal coordination and evaluate its adsorption capacity towards fluorocarbons and VOCs. The MOF synthesized in this work, $[\text{Zr}_6\text{O}_4(\text{OH})_4(\text{cca})_6]$ or Zr-cca (cca = 4-carboxycinnamate), is an analogue of UiO-66 but comprises a longer organic ligand.²⁷ We have done a comprehensive study on its synthesis, structure, stability, porosity, and adsorption toward various adsorbates. Zr-cca shows permanent porosity and high thermal/water stability. It exhibits highly favorable adsorption toward C_3 and C_4 hydrocarbons over C_2 hydrocarbons, as indicated by isosteric heat of adsorption and IAST adsorption selectivity calculations. We have also investigated its adsorption of VOCs and selected fluorocarbons, including perfluorohexane, a greenhouse species that has been used

extensively in cooling of the electronics and that has a 100-year GWP 9300 times higher than that of carbon dioxide.

EXPERIMENTAL SECTION

Materials and methods. All reagents were obtained from commercial sources and used without further purification. Single crystal X-ray diffraction data were collected on a D8 goniostat equipped with a Bruker PHOTON100 CMOS detector at Beamline 11.3.1 at the Advanced Light Source (Lawrence Berkeley National Laboratory) using synchrotron radiation. Powder X-ray diffraction patterns were recorded on a Ultima IV with Cu K α radiation ($\lambda = 1.5406 \text{ \AA}$). Data were collected at room temperature at $2\theta = 3\text{-}40^\circ$ with a scan speed of 2 deg/min and operating power of 40 kV and 44 mA. Thermogravimetric analysis was performed on a TA Q5000 analyzer. Around 2-5 mg of sample was heated from room temperature to 600 °C at a ramp rate of 10 °C/min. Gas adsorption measurements were carried out on a Micromeritics 3Flex volumetric adsorption analyzer. Liquid nitrogen and a circulating-bath digital temperature controller were used for measurements at 77 K and temperatures around room temperature, respectively. For each adsorption measurement, around 100 mg as synthesized sample was used and activated at 150 °C under dynamic vacuum overnight prior to adsorption experiments.

Isosteric heat of adsorption. The isosteric heat of adsorption for each gas was calculated from adsorption isotherms at three different temperatures (278, 288, and 298 K) using the virial method.²⁸ The isotherms were first fitted with virial equation:

$$\ln(p) = \ln(v) + (1/T) \sum_{i=0}^m a_i v^i + \sum_{j=0}^n b_j v^j$$

Where v , p , and T are adsorbed amount, pressure, and temperature, respectively. Isotheric heat of adsorption can be obtained with the fitting parameter through the following equation:

$$Q_{st} = -R \sum_{i=0}^g a_i v^i$$

Where R is the universal gas constant.

IAST adsorption selectivity. IAST adsorption selectivities were calculated following previously reported methods.^{18, 29} Single component adsorption isotherms (at room temperature) for each adsorbate were first fitted to the dual site Langmuir-Freundlich (DSLFF) model and the obtained parameters were used to calculate the adsorption selectivity between two components.

Material synthesis. Zr-cca was synthesized through solvothermal reaction. $ZrOCl_2 \cdot 8H_2O$ (64.4 mg, 0.2 mmol), benzoic acid (800 mg, 6.5 mmol) were ultrasonically dissolved in N,N-dimethylformamide (DMF, 10 mL) in a 20 mL glass vial. 4-carboxycinnamic acid (H_2cca , 38.4 mg, 0.2 mmol) was subsequently added to the solution and was then sonicated for 5 minutes before being placed in an oven. After heating at 120 °C for 3 days the reaction was cooled to room temperature. Colorless octahedral crystals were obtained through filtration.

UiO-66 was prepared according to reported procedure³⁰ and the phase purity was confirmed by powder X-ray diffraction and porosity characterization.

VOCs and fluorocarbon adsorption measurements. Adsorption experiments of selected VOCs and fluorocarbon were performed on a gravimetric adsorption unit modified from TA Q50 thermogravimetric analyzer. For each measurement, ~20 mg of as-synthesized Zr-cca sample was loaded onto the platinum pan and heated at 150 °C under nitrogen flow for 2 hours to remove any residues in the pores. After cooling down to 30 °C, another nitrogen flow passing through the VOC bubbler connected to a condenser maintained at 18 °C was mixed with the pure N₂ stream and then introduced to the adsorption chamber. Mass flow controllers were used to control the flow rates of the two gas streams in order to maintain the partial pressure of the adsorbate at certain level. Sample weight was recorded throughout the process, which dictates the uptake amount of adsorbate with respect to time. Sufficient time was given for the adsorption process to guarantee adsorption equilibrium was achieved under preset VOC concentration.

RESULTS AND DISCUSSION

Synthesis and crystal structure. Zr-cca was prepared solvothermally by heating a mixture of $\text{ZrOCl}_2 \cdot 8\text{H}_2\text{O}$, H_2cca and benzoic acid in DMF at 120 °C for 3 days (see experimental section for detailed synthesis). Octagon-shaped crystals suitable for single crystal X-ray diffraction were harvested. Structure analysis shows that Zr-cca crystallizes in the space group *Pn-3* (see Supporting Information Table S1 for detailed crystal data) with a formula of $\text{Zr}_6\text{O}_4(\text{OH})_4(\text{cca})_6$. Similar to many other Zr-MOFs built with linear dicarboxylate linkers, Zr-cca is isorecticular to UiO-66. The $\text{Zr}_6\text{O}_4(\text{OH})_4(\text{COO})_{12}$ SBU is connected to twelve adjacent SBUs through cca linkers. Two types of cages are found in the structure. One is tetrahedron with a pore size of ~6 Å and the other is octahedron with a pore size of ~8 Å (Figure 1). The structure and pore shape/size of Zr-

cca are similar to a recently reported zirconium MOF, DUT-52, built on 2,6-naphthalenedicarboxylate, which has similar length with cca.³¹

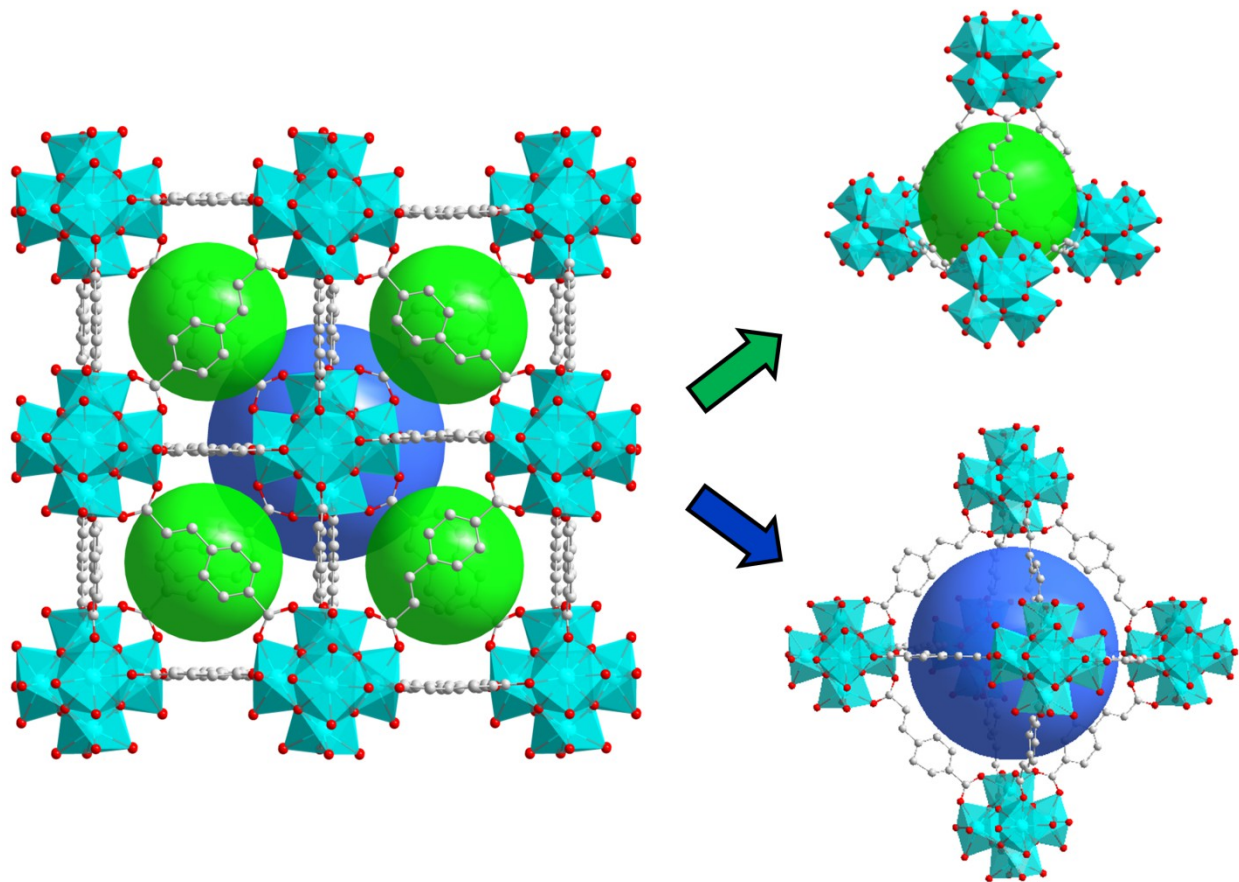


Figure 1. Crystal structure of Zr-cca. Green and blue spheres represent the tetrahedral and octahedral cages in the structure, respectively. Color scheme: cyan (Zr), red (O), grey (C). Hydrogen atoms are omitted for clarity.

As well recognized, acid modulators are usually necessary for the formation of crystalline Zr-MOFs. The exact role of these modulators remains unclear, and possible explanations were proposed from previous studies.³² Acid modulators may serve as a competing agent to coordinate with the metal thus slowing down the crystal growth rate to avoid fast precipitation of amorphous products, which allows the formation of large MOFs crystals. For the synthesis of Zr-

cca, different acids were used as modulators. Replacing benzoic acid with acetic acid as modulator resulted in the same phase, as indicated by PXRD analysis (denoted as Zr-cca-AA, see Supporting Information Figure S8). Interestingly, when formic acid was used, a different crystalline phase was obtained (denoted as Zr-cca-FA, See Supporting Information Figure S9). In spite of the tremendous efforts made in optimizing the reaction conditions, crystals large enough for single crystal X-ray diffraction analysis cannot be achieved for this phase. The porosity analysis on Zr-cca-FA showed negligible N₂ adsorption at 77 K so its permanent porosity was estimated by CO₂ adsorption at 273 K, which offered a BET surface area of 140 m²/g (Figure S13). This compound also exhibits high stability in aqueous solutions (Supporting Information Figure S11). Our results suggest that acid modulators may have served as templates in solvothermal reactions, since a different structure with reduced porosity was obtained when formic acid was used, an acidic modulator with smaller molecular size compared to benzoic or acetic acid. It should be noted that this observation represents a rare case where different acid modulators lead to different Zr-MOF structures.¹³

Porosity characterization and stability test. It is worth mentioning that Zr-cca can be fully activated by direct heating at 150 °C and no solvent exchange is needed. Nitrogen adsorption-desorption isotherm at 77 K was collected for Zr-cca in order to confirm its permanent porosity upon removal of solvent initially residing inside pores. The observed Type I adsorption profile indicates the microporous nature of the material (Figure 2). The BET surface area and total pore volume of Zr-cca are calculated to be 1178 m²/g and 0.48 cm³/g, respectively, based on nitrogen adsorption data collected at 77 K. Note these values are lower than those of UiO-66 which is made of a shorter linker ligand, bdc. We also noticed that the experimental BET values for both Zr-cca and DUT-52 are lower than their calculated value, which is ~ 1700 m²/g for both

structures assuming 12 linkers per metal node.³¹ While this discrepancy could be due to a number of reasons,³³ such as insufficient activation or partial structural degradation, we speculate that the difference in their structural defects (missing linkers) may also contribute partially to the observed porosity. UiO-66 is a well-known defect structure and the amount of missing linkers vary from 8% to as high as 50%, depending on the synthesis conditions.¹⁰ The calculated BET surface areas for UiO-66 are 800 m²/g and 1550 m²/g for a SBU connectivity of 12 and 8, respectively.³⁰ The UiO-66 sample tested in this work has an experimental BET surface area of 1240 m²/g, corresponding to an estimated 20% of missing linkers (defects)³⁰ while the value is ~10% for Zr-cca based on single crystal X-ray diffraction analysis. The pore size distribution curve of Zr-cca shows two peaks centered at ~ 6 Å and ~ 8 Å, respectively, which is in excellent agreement with the pore size measured based on its crystal structure.

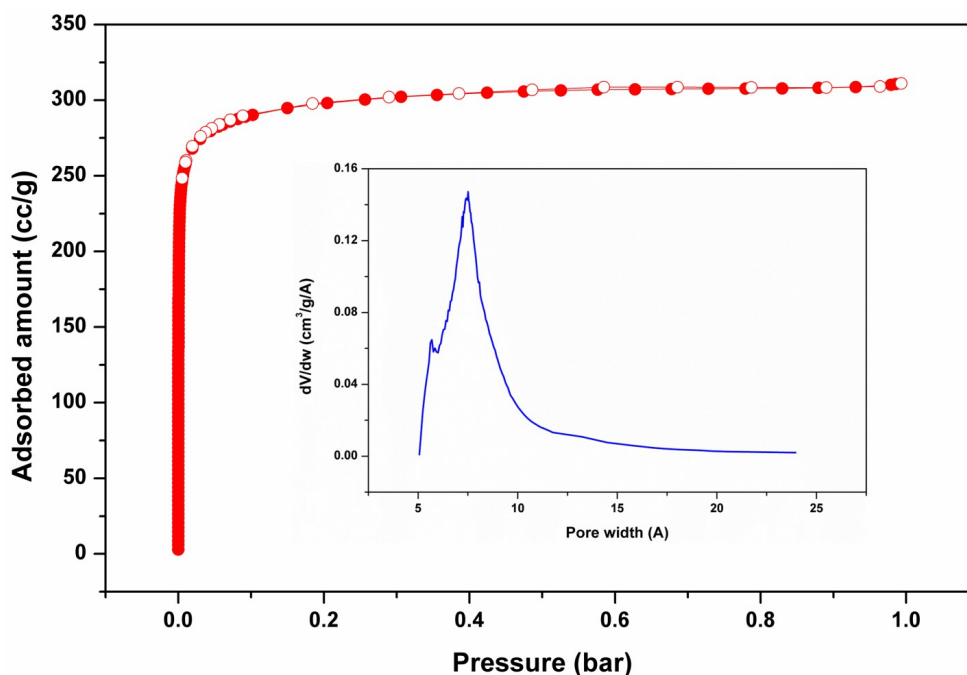
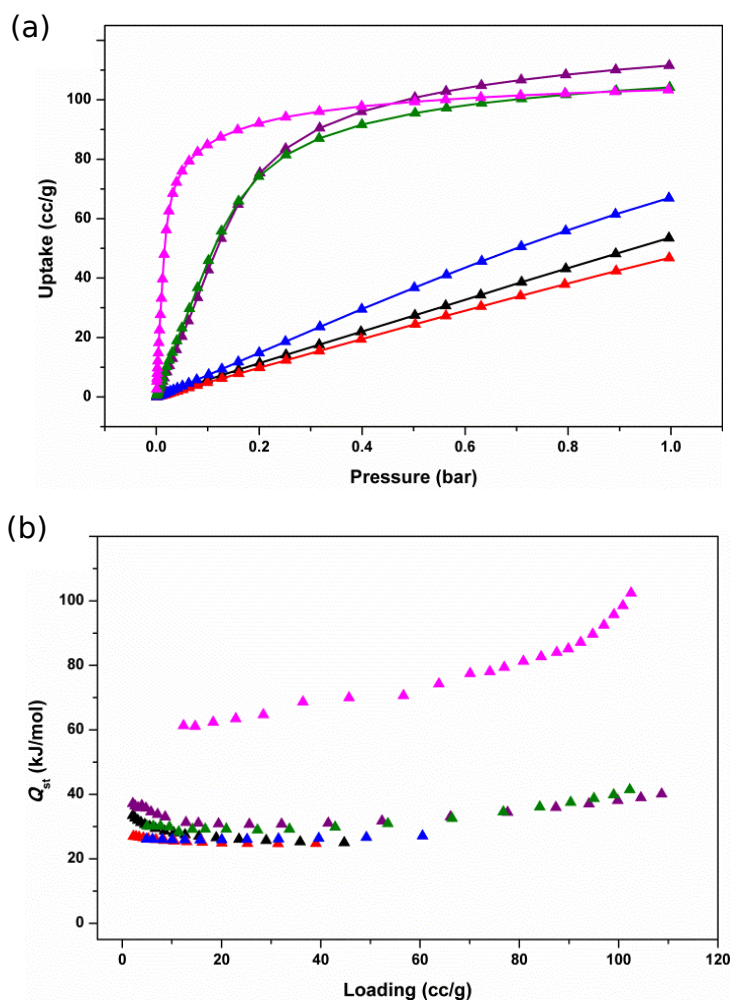


Figure 2. Nitrogen adsorption-desorption isotherm at 77 K for Zr-cca. Insert: pore size distribution.

Zr-cca shows high thermal and water stability. This once again proves that the utilization of early transition metals is an effective way to enhance the stability of MOFs. Zr-cca maintained its crystallinity after being heated at 300 °C for 24 hours in open air (Supporting Information Figure S6). Moreover, no structural change was observed for Zr-cca after being immersed in aqueous solutions with a wide range of pH values (0 – 11), indicating its high resistance toward aqueous or acidic/basic conditions (Supporting Information Figure S7).



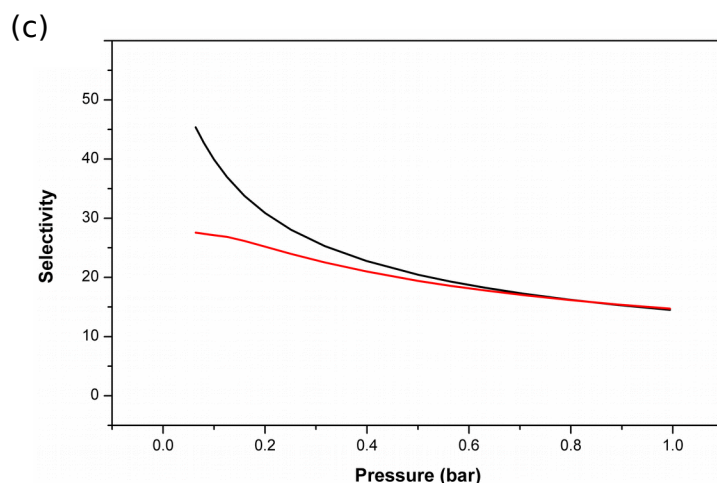


Figure 3. (a) Adsorption isotherms at 298 K and (b) Isothermic heat of adsorption of acetylene (black), ethylene (red), ethane (blue), propylene (purple), propane (olive), and n-butane (magenta) in Zr-cca. Desorption branches were omitted for clarity. (c) n-butane/ethane (black) and propane/ethane (red) IAST selectivity of equimolar binary mixtures at 298 K.

Hydrocarbon adsorption. Since separation between light hydrocarbons is of high importance in industrial applications, we studied the adsorption behavior of Zr-cca toward light hydrocarbons (C_2 - C_4). For example, natural gas liquids (NGLs) are currently a growing supply as feedstocks for fuel and the chemical industry. Adsorptive-based separation can act as an alternative or supplement to improve the efficiency of NGLs separation currently undertaken by energy-intensive cryogenic distillation.³⁴ In addition, NGLs separation by MOFs has not been extensively explored so far.¹⁹ We collected adsorption-desorption isotherms of six light hydrocarbons (acetylene, ethylene, ethane, propane, propylene and n-butane, see Figure S15) at three different temperatures (278, 288 and 298 K) and calculated the isosteric heat of adsorption (Q_{st}) for each gas based on these isotherm data. Both adsorbed amount and adsorption affinity increase from C_2 to C_4 hydrocarbons, as indicated by the shape of the adsorption isotherms and

Q_{st} (Figure 3). The uptake of C_2 , C_3 , and C_4 hydrocarbons at 1 bar and room temperature are 5.9 – 9.0 wt%, ~20 wt% and 26.7 wt%, respectively. The isosteric heat of adsorption for C_2 hydrocarbons are ~ 25 kJ/mol while the values for C_3 and C_4 hydrocarbons are ~30 and ~60 kJ/mol, respectively. It is observed that the Q_{st} values increase as the number of carbons increases from two to four, as commonly seen in other cases.²⁰ We believe that this is because larger molecular size of adsorbates leads to stronger van der Waals interaction with the pore surface of the adsorbent. Ideal adsorbed solution theory (IAST) was used to estimate the adsorption selectivity of C_3 and C_4 hydrocarbons over C_2 hydrocarbons. As shown in Figure 3c, adsorption selectivity of n-butane/ethane and propane/ethane of equimolar binary mixtures at 298 K decrease as total pressure increase and reach a steady value of ~ 18 when total pressure approaches to 1 bar in both cases. These high selectivity values are consistent with the single component adsorption isotherms and isosteric heat of adsorption results.

Liquid hydrocarbons with high vapor pressure belong to the class of volatile organic compounds (VOCs). We tested Zr-cca for the adsorption of common hydrocarbon VOCs such as n-pentane, hexane isomers, and xylene isomers. The adsorption experiments were performed on a home-modified thermogravimetric adsorption analyzer. Nitrogen was used as a carrier gas which flows through a bubbler containing the liquid adsorbate and introduces the vapor into the furnace where MOF sample was located and sample weight was monitored. As shown in Figure S17, at 30 °C, Zr-cca takes up 20 – 35 wt% of these hydrocarbon VOCs. It was observed that the adsorption rate decreases as the molecular size of the adsorbates increases. This is because the size of large adsorbates such as 1,3,5-trimethylbenzene is approaching the pore size of Zr-cca.

Adsorption of perfluorohexane. Perfluoroalkanes are widely used as refrigerants, anesthetics, as well as for many other industrial purposes. However, due to their long lifetime in the

atmosphere, perfluoroalkanes are potent greenhouse gases with much higher GWP than carbon dioxide. Capture of perfluorocarbons with porous sorbent materials has been proposed and tested with highly fluorinated structures specifically, since the fluoro decoration could potentially enhance the affinity between perfluoroalkanes and the sorbent. However these compounds are difficult to prepare and lack of robustness.²⁴ Here we have attempted to use Zr-cca for the capture of perfluoroalkane considering its relatively high porosity, excellent stability and facile preparation. We selected perfluorohexane (PFC6) as a probe molecule because it is widely used for low-temperature applications but has been identified as a potent greenhouse species with very high GWP. The measurement was carried out in a similar method applied to VOCs adsorption experiments. As shown in Figure 4a, Zr-cca was able to take up more than 50 wt% of perfluorohexane at 30 °C within a couple of minutes upon exposure to the perfluorohexane vapor. When the feed gas was switched from N₂ and PFC6 mixture to pure N₂, desorption began to occur but slowly. However, when slight heating was applied, the adsorbed PFC6 was removed rapidly and desorption quickly reached completion. The adsorption-desorption cycle was repeated 10 times consecutively and the adsorption capacity was fully maintained after 10 cycles (Figure 4b). Although Zr-cca does not have the highest PFC6 adsorption capacity, its facile synthesis, excellent thermal and water stability, good recyclability render it a strong candidate for adsorption and sequestration of PFC6.

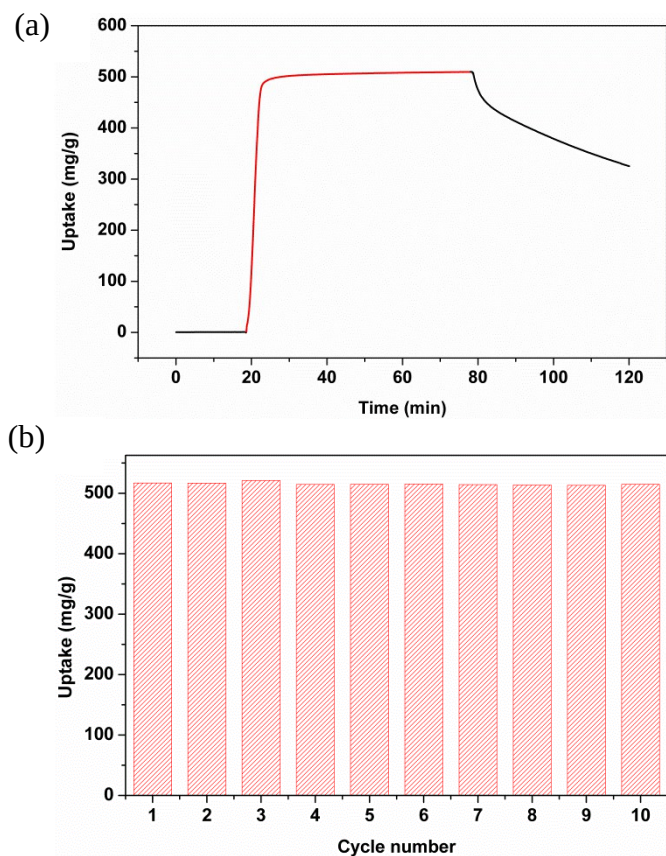


Figure 4. (a) Adsorption-desorption curve of perfluorohexane on Zr-cca at 30 °C. Black and red curves indicate pure nitrogen and a mixture of nitrogen and perfluorohexane vapor (partial pressure: 20 kPa) as feed gases, respectively. (b) Perfluorohexane adsorption cycles on Zr-cca. Desorption was carried out at 100°C for 30 min under nitrogen.

For comparison purpose, we also collected perfluorohexane adsorption data on UiO-66. Interestingly, while UiO-66 has a larger experimental BET surface area, it only adsorbs 45 wt% of perfluorohexane under the same experimental conditions, which is lower than that of Zr-cca (51 wt%). We speculate that this is because Zr-cca is more hydrophobic as a result of lower degree of ligand defect (i.e. less amount of missing linkers), which in turn increases its affinity for perfluorohexane. In order to confirm this hypothesis, we performed adsorption measurements

of normal octane on both UiO-66 and Zr-cca at high temperatures (100, 110, 120, and 130 °C) and calculated the isosteric heat of adsorption using these data. It is clearly visible that the adsorption isotherms for Zr-cca are steeper than those for UiO-66, indicating a stronger affinity for the former. The calculated isosteric heats of adsorption of normal octane are 64 and 55 kJ/mol, for Zr-cca and UiO-66, respectively, again supporting the above hypothesis. The above results indicate the possibility of regulating the amount of missing linkers in order to control the MOF hydrophobicity.

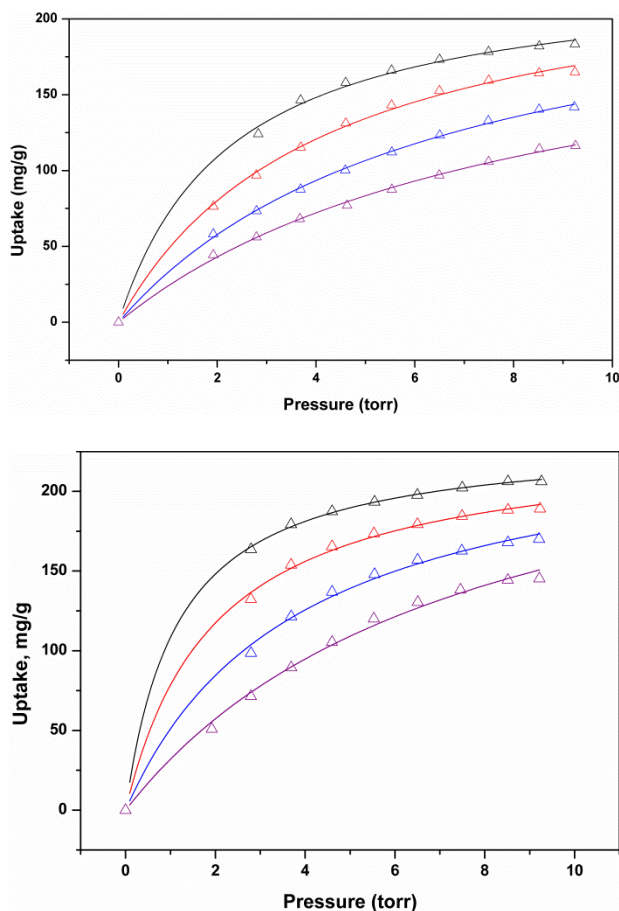


Figure 5. n-octane adsorption isotherms on UiO-66 (top) and Zr-cca (bottom) at 100 °C (black), 110 °C (red), 120 °C (blue), and 130 °C (purple).

CONCLUSION

In conclusion, we have successfully grown single crystals of $[\text{Zr}_6\text{O}_4(\text{OH})_4(\text{cca})_6]$ (Zr-cca), a UiO-66 analogue, using a less symmetric 4-carboxycinnamic acid as the organic linker. Different acid modulators were tested for the solvothermal synthesis reactions. Zr-cca exhibits high thermal/water stability and permanent porosity. It shows selective adsorption toward C_3 and C_4 over C_2 hydrocarbons with high selectivity. Adsorption of selected VOCs and perfluoroalkane in Zr-cca shows that it takes up more than 50 wt% of perfluorohexane at 30 °C with excellent recyclability. A comparison between Zr-cca and UiO-66 reveals a reverse relationship on the MOF BET values and perfluorohexane loading amounts. A possible underlying reason is elucidated based on the difference in the extent of ligand defects and related hydrophobicity. This study suggests that stable, highly porous and site-modifiable MOFs can be designed for selected capture and sequestration of VOCs and fluorocarbons.

ASSOCIATED CONTENT

The supporting Information is available free of charge on the ACS Publications website at DOI: Powder X-ray diffraction (PXRD) patterns, thermogravimetric analysis (TGA) results, adsorption isotherms for various adsorbates, material stability test (PDF).

ACKNOWLEDGEMENTS

This study is supported by the U.S. Department of Energy (DOE), Office of Basic Energy Sciences, Materials Sciences and Engineering Division through grant no. DE-FG02-08ER46491. The Advanced Light Source is supported by the Director, Office of Science, Office of Basic Energy Sciences, of the U.S. Department of Energy under Contract No. DE-AC02-05CH11231.

We would also like to acknowledge Micromeritics Instrument Corp. for the donation of a new 3Flex system through its Instrument Grant program.

REFERENCES

- 1 Zhou, H.-C.; Long, J. R. Yaghi, O. M., Introduction to Metal–Organic Frameworks, *Chem. Rev.* **2012**, *112*, 673-674.
- 2 Wu, H.; Gong, Q.; Olson, D. H. Li, J., Commensurate Adsorption of Hydrocarbons and Alcohols in Microporous Metal Organic Frameworks, *Chem. Rev.* **2012**, *112*, 836-868.
- 3 Sumida, K.; Rogow, D. L.; Mason, J. A.; McDonald, T. M.; Bloch, E. D.; Herm, Z. R.; Bae, T.-H. Long, J. R., Carbon Dioxide Capture in Metal–Organic Frameworks, *Chem. Rev.* **2012**, *112*, 724-781.
- 4 Zeng, L.; Guo, X.; He, C. Duan, C., Metal–Organic Frameworks: Versatile Materials for Heterogeneous Photocatalysis, *ACS Catal.* **2016**, *6*, 7935-7947.
- 5 Hu, Z.; Deibert, B. J. Li, J., Luminescent metal-organic frameworks for chemical sensing and explosive detection, *Chem. Soc. Rev.* **2014**, *43*, 5815-5840.
- 6 Lan, A.; Li, K.; Wu, H.; Olson, D. H.; Emge, T. J.; Ki, W.; Hong, M. Li, J., A Luminescent Microporous Metal–Organic Framework for the Fast and Reversible Detection of High Explosives, *Angew. Chem. Int. Ed.* **2009**, *48*, 2334-2338.
- 7 Pramanik, S.; Zheng, C.; Zhang, X.; Emge, T. J. Li, J., New Microporous Metal–Organic Framework Demonstrating Unique Selectivity for Detection of High Explosives and Aromatic Compounds, *J. Am. Chem. Soc.* **2011**, *133*, 4153-4155.
- 8 Gong, Q.; Hu, Z.; Deibert, B. J.; Emge, T. J.; Teat, S. J.; Banerjee, D.; Mussman, B.; Rudd, N. D. Li, J., Solution Processable MOF Yellow Phosphor with Exceptionally High Quantum Efficiency, *J. Am. Chem. Soc.* **2014**, *136*, 16724-16727.
- 9 Hu, Z.; Huang, G.; Lustig, W. P.; Wang, F.; Wang, H.; Teat, S. J.; Banerjee, D.; Zhang, D. Li, J., Achieving exceptionally high luminescence quantum efficiency by immobilizing

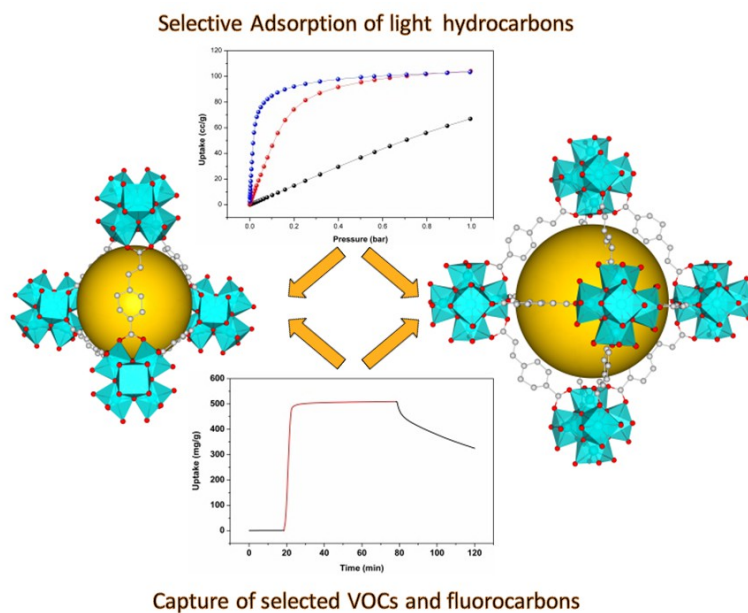
- an AIE molecular chromophore into a metal-organic framework, *Chem. Commun.* **2015**, *51*, 3045-3048.
- 10 Trickett, C. A.; Gagnon, K. J.; Lee, S.; Gándara, F.; Bürgi, H.-B. Yaghi, O. M., Definitive Molecular Level Characterization of Defects in UiO-66 Crystals, *Angew. Chem. Int. Ed.* **2015**, *54*, 11162-11167.
- 11 Kizzie, A. C.; Wong-Foy, A. G. Matzger, A. J., Effect of humidity on the performance of microporous coordination polymers as adsorbents for CO₂ capture, *Langmuir* **2011**, *27*, 6368-6373.
- 12 Burtch, N. C.; Jasuja, H. Walton, K. S., Water stability and adsorption in metal-organic frameworks, *Chem. Rev.* **2014**, *114*, 10575-10612.
- 13 Bai, Y.; Dou, Y.; Xie, L.-H.; Rutledge, W.; Li, J.-R. Zhou, H.-C., Zr-based metal-organic frameworks: design, synthesis, structure, and applications, *Chem. Soc. Rev.* **2016**.
- 14 Cavka, J. H.; Jakobsen, S.; Olsbye, U.; Guillou, N.; Lamberti, C.; Bordiga, S. Lillerud, K. P., A New Zirconium Inorganic Building Brick Forming Metal Organic Frameworks with Exceptional Stability, *J. Am. Chem. Soc.* **2008**, *130*, 13850-13851.
- 15 Peng, Y.; Krungleviciute, V.; Eryazici, I.; Hupp, J. T.; Farha, O. K. Yildirim, T., Methane Storage in Metal–Organic Frameworks: Current Records, Surprise Findings, and Challenges, *J. Am. Chem. Soc.* **2013**, *135*, 11887-11894.
- 16 He, Y.; Zhou, W.; Qian, G. Chen, B., Methane storage in metal-organic frameworks, *Chem. Soc. Rev.* **2014**, *43*, 5657-5678.
- 17 Xiang, S.; He, Y.; Zhang, Z.; Wu, H.; Zhou, W.; Krishna, R. Chen, B., Microporous metal-organic framework with potential for carbon dioxide capture at ambient conditions, *Nat. Commun.* **2012**, *3*, 954.

- 18 Zhang, Z.; Zhao, Y.; Gong, Q.; Li, Z. Li, J., MOFs for CO₂ capture and separation from flue gas mixtures: the effect of multifunctional sites on their adsorption capacity and selectivity, *Chem. Commun.* **2013**, *49*, 653-661.
- 19 Wang, H.; Wang, X.-L. Li, J., Separation of Light Hydrocarbons through Selective Molecular Exclusion by a Microporous Metal–Organic Framework, *ChemPlusChem* **2016**, *81*, 872-876.
- 20 Herm, Z. R.; Bloch, E. D. Long, J. R., Hydrocarbon Separations in Metal–Organic Frameworks, *Chem. Mater.* **2014**, *26*, 323-338.
- 21 Wang, H.; Yao, K.; Zhang, Z.; Jagiello, J.; Gong, Q.; Han, Y. Li, J., The first example of commensurate adsorption of atomic gas in a MOF and effective separation of xenon from other noble gases, *Chem. Sci.* **2014**, *5*, 620-624.
- 22 Banerjee, D.; Simon, C. M.; Plonka, A. M.; Motkuri, R. K.; Liu, J.; Chen, X.; Smit, B.; Parise, J. B.; Haranczyk, M. Thallapally, P. K., Metal–organic framework with optimally selective xenon adsorption and separation, *Nat. Commun.* **2016**, *7*, ncomms11831.
- 23 Banerjee, D.; Cairns, A. J.; Liu, J.; Motkuri, R. K.; Nune, S. K.; Fernandez, C. A.; Krishna, R.; Strachan, D. M. Thallapally, P. K., Potential of Metal–Organic Frameworks for Separation of Xenon and Krypton, *Acc. Chem. Res.* **2015**, *48*, 211-219.
- 24 Chen, T.-H.; Popov, I.; Kaveevivitchai, W.; Chuang, Y.-C.; Chen, Y.-S.; Jacobson, A. J. Miljanić, O. Š., Mesoporous Fluorinated Metal–Organic Frameworks with Exceptional Adsorption of Fluorocarbons and CFCs, *Angew. Chem. Int. Ed.* **2015**, *54*, 13902-13906.
- 25 Chen, T.-H.; Popov, I.; Kaveevivitchai, W.; Chuang, Y.-C.; Chen, Y.-S.; Daugulis, O.; Jacobson, A. J. Miljanić, O. Š., Thermally robust and porous noncovalent organic framework with high affinity for fluorocarbons and CFCs, *Nat. Commun.* **2014**, *5*.

- 26 Senkovska, I.; Barea, E.; Navarro, J. a. R.Kaskel, S., Adsorptive capturing and storing greenhouse gases such as sulfur hexafluoride and carbon tetrafluoride using metal-organic frameworks, *Micro. Meso. Mater.* **2012**, *156*, 115-120.
- 27 Sk, M.; Grzywa, M.; Volkmer, D.Biswas, S., Zr(IV) and Ce(IV)-based metal-organic frameworks incorporating 4-carboxycinnamic acid as ligand: Synthesis and properties, *Micro. Meso. Mater.* **2017**, *237*, 275-281.
- 28 Czepirski, L.Jagiełło, J., Virial-type thermal equation of gas—solid adsorption, *Chem. Eng. Sci* **1989**, *44*, 797-801.
- 29 Zhang, Z.; Liu, J.; Li, Z.Li, J., Experimental and theoretical investigations on the MMOF selectivity for CO₂vs. N₂ in flue gas mixtures, *Dalton Trans.* **2012**, *41*, 4232-4238.
- 30 Katz, M. J.; Brown, Z. J.; Colon, Y. J.; Siu, P. W.; Scheidt, K. A.; Snurr, R. Q.; Hupp, J. T.Farha, O. K., A facile synthesis of UiO-66, UiO-67 and their derivatives, *Chem. Commun.* **2013**, *49*, 9449-9451.
- 31 Bon, V.; Senkovska, I.; Weiss, M. S.Kaskel, S., Tailoring of network dimensionality and porosity adjustment in Zr- and Hf-based MOFs, *CrystEngComm* **2013**, *15*, 9572-9577.
- 32 Hu, Z.; Castano, I.; Wang, S.; Wang, Y.; Peng, Y.; Qian, Y.; Chi, C.; Wang, X.Zhao, D., Modulator Effects on the Water-Based Synthesis of Zr/Hf Metal–Organic Frameworks: Quantitative Relationship Studies between Modulator, Synthetic Condition, and Performance, *Cryst. Growth Des.* **2016**, *16*, 2295-2301.
- 33 Decoste, J. B.; Peterson, G. W.; Jasuja, H.; Glover, T. G.; Huang, Y.-G.Walton, K. S., Stability and degradation mechanisms of metal-organic frameworks containing the Zr₆O₄(OH)₄ secondary building unit, *Journal of Materials Chemistry A* **2013**, *1*, 5642-5650.

- 34 Pimentel, B. R.Lively, R. P., Enabling Kinetic Light Hydrocarbon Separation via Crystal Size Engineering of ZIF-8, *Ind. Eng. Chem. Res.* **2016**, 55, 12467-12476.

For Table of Contents Only



A single crystalline zirconium based MOF has been synthesized and characterized. With microporosity and high thermal and water stability, the Zr-MOF shows selective adsorption of light hydrocarbons. Its adsorption performance toward selected VOCs and fluorocarbon is also evaluated.